Journal of Engineering Research and Applied Science
Available at www.journaleras.com
Volume 11 (2), December 2022, pp 2093-2103
ISSN 2147-3471 © 2022

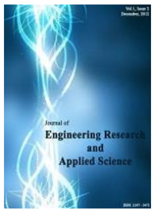

Textural features of Eocene-aged sandstones from Gümüşhane (NE Türkiye): Evidence from grain size analysis

Cigdem Saydam Eker

Gumushane University, Engineering and Natural Sciences Faculty, Geology, Gumushane, Turkey

Accepted 18 November 2022

Abstract

In the present study, a total of 15 characteristic sandstone samples of Eocene siliciclastic rocks in the Kelkit (Gumushane) area have been examined for their grain size textural parameters. The siliciclastic rocks are generally composed of thin – thick-bedded, light grey, brown-colored sandstones and thin, medium bedded, green, yellowish-brown, greenish grey colored marl intercalated. The mean grain size (Mz) of the sandstone samples ranges from 1.93 to 2.77 ϕ) and is classified as medium-grained - fine-grained sandstone. The Standard deviation (σ1) values of the sample are between 0.27 and 1.07 ϕ and the sandstone samples' sorting range from very well-sorted to poorly sorted. The calculated graphic skewness (Sk) values for sandstone samples range from -0.2 to 0.16 ϕ and are categorized as coarse-skewed and fine-skewed. According to the morphology of grains, the sandstone samples were defined as subangular, subrounded, and rounded. Based on the textural parameter data, Eocene-aged sandstones in the studied area mainly change between texturally mature and immature sandstones. The sandstones are thought to have taken material from bivariate sources, one closer to the basin and the other farther away.

Keywords: Sandstone, Textural characteristic, Grain size, Sorting, Skewed, Grain morphology

1. Introduction

Siliciclastic rocks are various groups of sedimentary rocks, that change from coarse-grained conglomerate, through sandstones to fine-grained mudstones. These rocks are generally composed of fragments and minerals, originating from older sedimentary, igneous, and metamorphic rocks. Siliciclastic rocks have two significant features of sedimentary textures and structures, and most of them are produced by the depositional processes [1].

Textures (grain shape, roundness, and grain size) are important properties of sandstones used to understand the depositional environment and type of transport they experienced. These properties allow for determining the textural maturity of a sandstone [2]. Grain size analysis is particularly a beneficial parameter used by researchers on sandstones to acquire an exhaustive understanding of the paleoenvironmental properties and hydrodynamic conditions [3-5]. Since the size of grains in a sandstone brings to light their transportation processes and hydrodynamic energy, grain size distribution is one of the most important features of sandstones [6].

Eocene-aged rocks of the Gümüşhane region are observed in different lithology and source characteristics such as siliciclastic, volcaniclastic, volcanic, and plutonic rocks. These rocks were previously studied by different researchers for different purposes [7-15]. In this study, I present a detailed textural analysis of Eocene sandstones and discuss the source rock distance on sandstone textures dependent on main grain size (Mz), graphic skewness (Sk), and graphic sorting (σ1).

2. Geological setting

The basement of the Gümüşhane region includes Carboniferous granitoid and metamorphic massive [16-21]. The Carboniferous age rocks unconformably covered by the lower and middle Jurassic sequences are characterized by volcanic rocks (andesite and basalt) and plutonic rocks [22], sedimentary rocks represented by a conglomerate, sandstone, marl, shale, chert, and limestone [23-26]. The late Jurassic to middle Cretaceous age micritic, oolitic, sparitic, bituminous carbonates, and dolomite [27-28], conformably overlain the Jurassic rocks. The late Cretaceous rocks are represented by micritic limestone, sandy limestone, turbidites [29-30], volcanic rocks [31-33], and plutonic rocks [34-37] in

Corresponding author:
Email: csaydam@gumushane.edu.tr

the Gümüşhane region. Eocene-age rocks contain sedimentary rocks characterized by turbidites [7-8], plutonic rocks [38-39, 21], volcanic rocks [40-41, 13-14], and volcanic-clastic covering discordantly underlying rocks (Fig. 1). Quaternary sequences are represented by alluvium and travertine, the formation of which still continues [42-43].

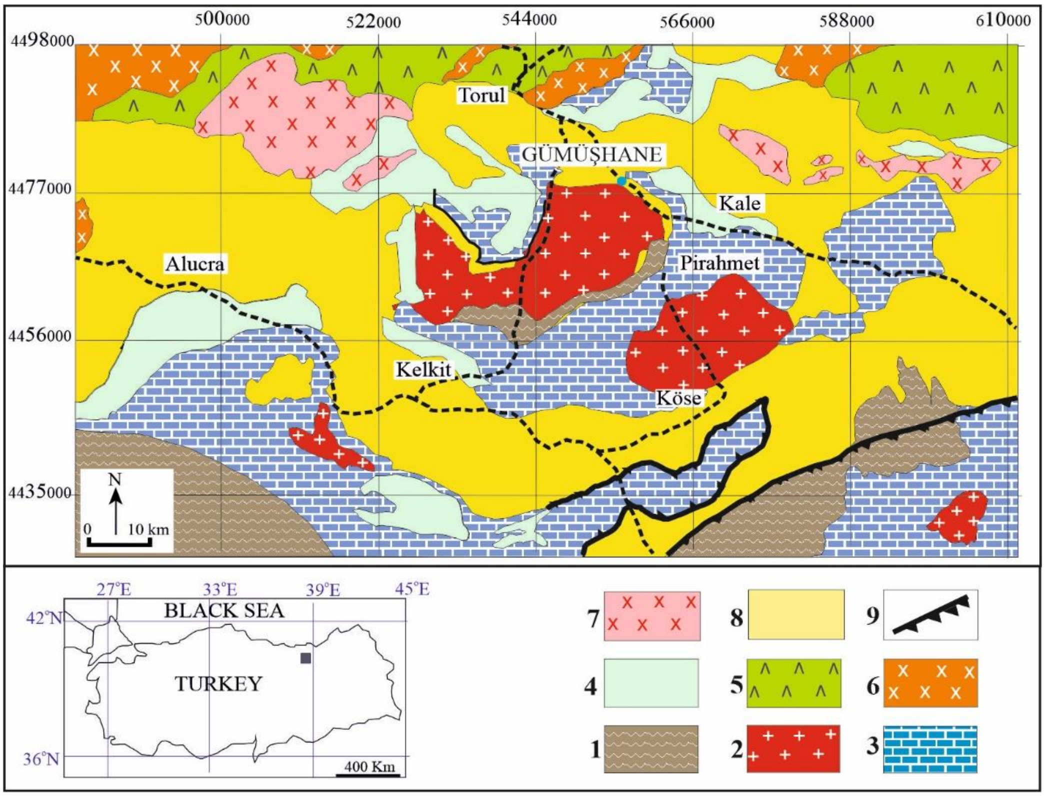

Figure 1. Geological and location map of the study area (simplified from Güven [44]) (1- Carboniferous metamorphic massive, 2- Carboniferous plutons, 3- Jurassic-early Cretaceous volcano-sedimentary sequence and carbonate rocks, 4- Late Cretaceous sedimentary rocks, 5- Late Cretaceous volcanic rocks, 6- Late Cretaceous plutons, 8- Eocene volcanic, volcano-sedimentary, sedimentary sequences. 9- Fault.

3. Materials and Methods

A stratigraphic section was measured from the Eocene-aged siliciclastic sequence a round north of Kelkit area and 15 sandstone samples were collected from the surface outcrop. Grain size data of sandstones are thought to be beneficial in interpreting the depositional environments of siliciclastic rocks. In the present study, 15 characteristics of thin sections of various sandstone types from the measured stratigraphic section were selected systematically for textural variations such as grain size and shape. The samples were examined for their grain size parameters. Grain size analysis was applied on the thin sections under a petrographic microscope with an inbuilt ocular millimeter scale. Generally, 500 grains were measured per thin section by using the standard method of measuring the longest axis of grain [45]. Grains in sandstones indicate a wide range of size distributions; Therefore, the frequencies of grain size ranges were computed, and the Udden–Wentworth grade scale was used to define the grain size classes. The unit of grain sizes (millimeters) was changed to a phi (ϕ) scale using the formula follow:

$\phi = -\mathrm{Log}_2 D$

Where ϕ represented the phi size and D represented the grain diameter in millimeters.

4. Result and discussion

4.1. Lithological and sedimentological features

Eocene-aged siliciclastic rocks lie over late Cretaceous-aged units which comprise red-colored micritic limestone, yellow-colored sandy limestone, and turbiditic rocks, with conformably in Kelkit (Gümüşhane). The thickness of the Eocene-aged siliciclastic rock was measured as 280 m in the Kelkit area from Gümüşhane (beginning X= 4448125, Y=537350 and finish X=4444775, Y=538950). The unit starts with gray-colored, coarse-grained, medium-bedded sandstone in the area and the features continue in the same way up to 9 m. There is a conglomerate layer approximately 2 m thick in the 9^{th} m, containing well-rounded pebbles of different lithologies with a diameter of 1-5 cm. This is overlain by very thin-medium bedded yellowish-brown sandstone. Upwards, the succession ends with an interbedded of thin-thick bedded, light gray, brown sandstone and thin, medium bedded, green, greenish gray, yellowish brown marl. The interbedded is accompanied by light gray thin, medium bedded limestone and tuff. Graded bedding and parallel lamination were observed as sedimentary structures in the sequence [46-47]. The sedimentary structures occur in the beds deposited by turbidity currents, exhibiting high and low-density flows. Graded bedding attached to grain sizes changes upwards through a bed and constantly improves in reaction to varieties in flow ceases during deposition. Reverse-graded bedding is a representative feature of turbidites deposited from accelerating density currents, whereas normal-graded bedding is a characteristic feature of turbidites deposited from waning density currents [1].

4.2. Textural features

The texture of a siliciclastic rock is generally an impact of the sedimentation process and so many siliciclastic rocks have been studied to define their textural characteristics, which contain grain size parameters, grain size, and grain morphology [1].

4.2.1. Grain-size parameters

Several grain-size parameters such as mean grain size, median grain size, mode, skewness, and sorting (Table 1) have been commonly used to determine sediment texture features. Calculating grain-size parameters are a routine procedure in many sedimentary studies, to introduce sediment and give information on its depositional environment and transport mechanism.

Table 1. Formulas for graphical calculation of grain size parameters [48].

Mean grain size (Mz)	$Mz = \frac{\phi16 + \phi50 + \phi84}{3}$
Graphic standard deviation (σ)	$\sigma = \frac{\phi84 - \phi16}{4} + \frac{\phi95 - \phi5}{6.6}$
Graphic skewness (Sk)	$Sk = \frac{\phi84 + \phi16 - 2\phi50}{2(\phi84 - \phi16)} + \frac{\phi95 + \phi5 - 2\phi50}{2(\phi95 - \phi5)}$

The 5th, 16th, 25th, 50th, 75th, 84th and 95th percentile on the cumulative frequency curve is represented by Ø5, Ø16, Ø25, Ø50, Ø75, Ø84, and Ø95, respectively.

4.2.2. Grain size

The basic illustrative parameter of sandstones is the grain size. There are too many grain-size scales but one which is commonly admitted and used is that of Udden and Wentworth [48]. In this study, the Udden – Wentworth scale was used to define grain size. The mean grain size (Mz) of the examined sandstones varies between 1.93 and 2.77 ϕ (Table 2) and is classified as medium-grained to fine-grained sandstone (Table 3). The grain size of the roof components (Quartz: monocrystalline and polycrystalline quartz, feldspar: Alkali feldspar and plagioclase, and rock fragment: volcanic rock fragment and sedimentary rock fragment) of the sandstones is slightly different. The grain size of monocrystalline quartz ranges from 3.27 ϕ (very fine sand) to -0.25 ϕ (very coarse sand) and polycrystalline quartz range from 3.13 ϕ (very fine sand) to -0.54 ϕ (very coarse sand). The grain size of alkali feldspar is between 3.25 ϕ (very fine sand) and -0.35 ϕ (very coarse sand) and plagioclase is between 3.63 ϕ (very fine sand) and 2.32 ϕ (fine sand). The grain size of volcanic rock fragments changes from 3.55 ϕ (very fine sand) to -0.41 ϕ (very coarse sand) and sedimentary rock fragments changes from 0.35 ϕ (coarse sand) to 3.05 ϕ (very fine sand) [46].

4.2.3. Graphic sorting

Sorting is a measure of standard deviation (σ_1) such as the spread of the grain-size distribution. The standard deviation (σ_1) is a very commonly used parameter since it ensures a sign of the influence of the depositional medium in separating grains of different classes [48]. The smoothed frequency curve and histogram indicate the frequency of grains in each size class and beneficial give the effect of the grain-size distribution, significantly as to whether a distribution is bimodal or unimodal. The cumulative frequency curve exhibits the percentage frequency of grains coarser than a particular value [1]. If the sorting is well, the frequency curve will be bell-shaped and the cumulative frequency curve will be S-shaped.

The standard deviation values of the studied sandstone sample vary from 0.27 to 1.07 ϕ (Table 3). According to these values, the sorting of sandstone samples is between very well-sorted and poorly sorted (Table 4). Figure 2 supports this classification because, in Figures 2f, k, and o, the curve shows a narrow distribution, while others show a wide distribution. It is possible to see a similar situation in the cumulative frequency curve. While the cumulative frequency curve in Figures 3f, k, and o are like the smooth "S", in other Figures the curve diverges from "S".

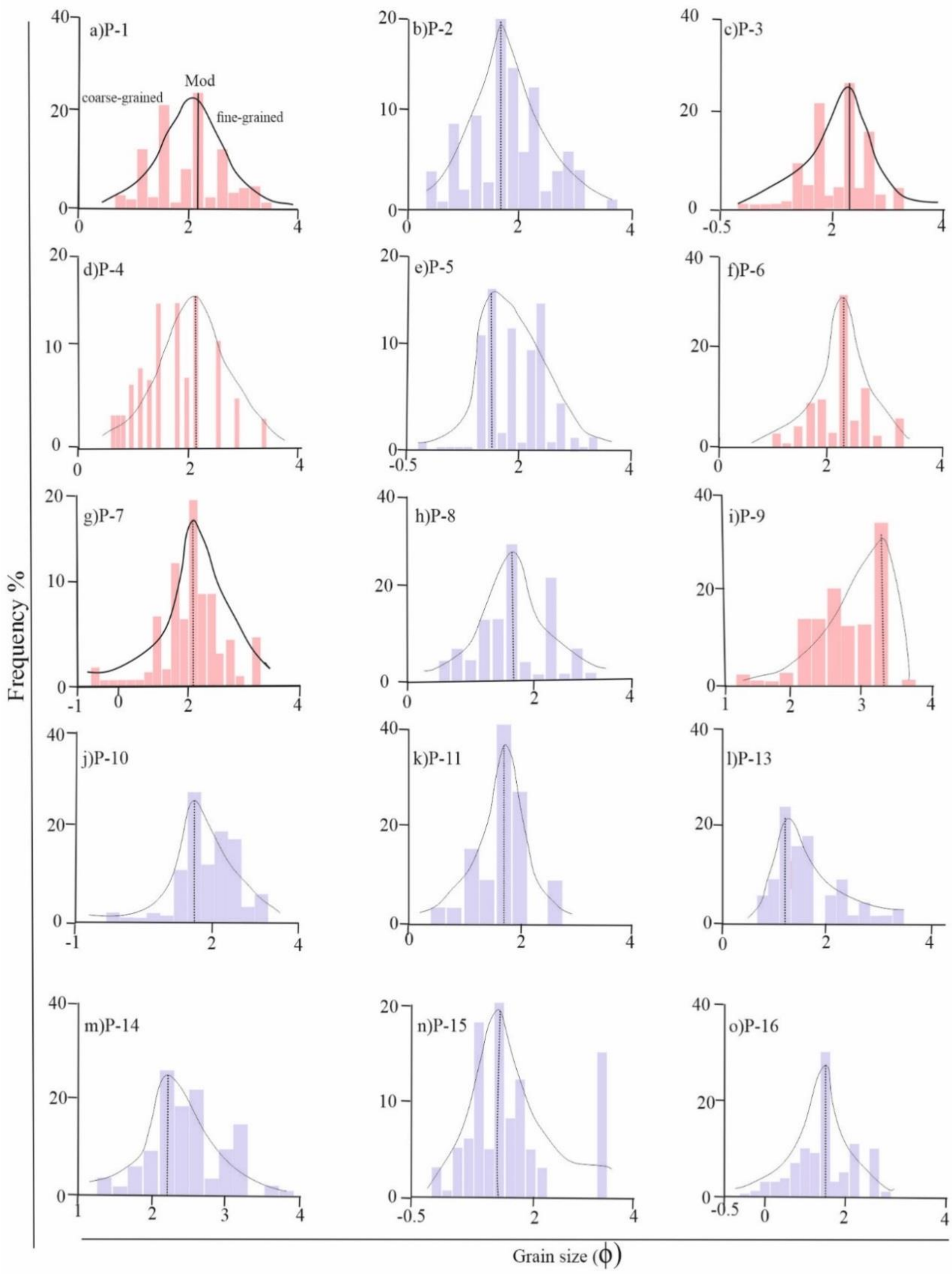

Figure 2. Histograms and frequency curves of the sandstones

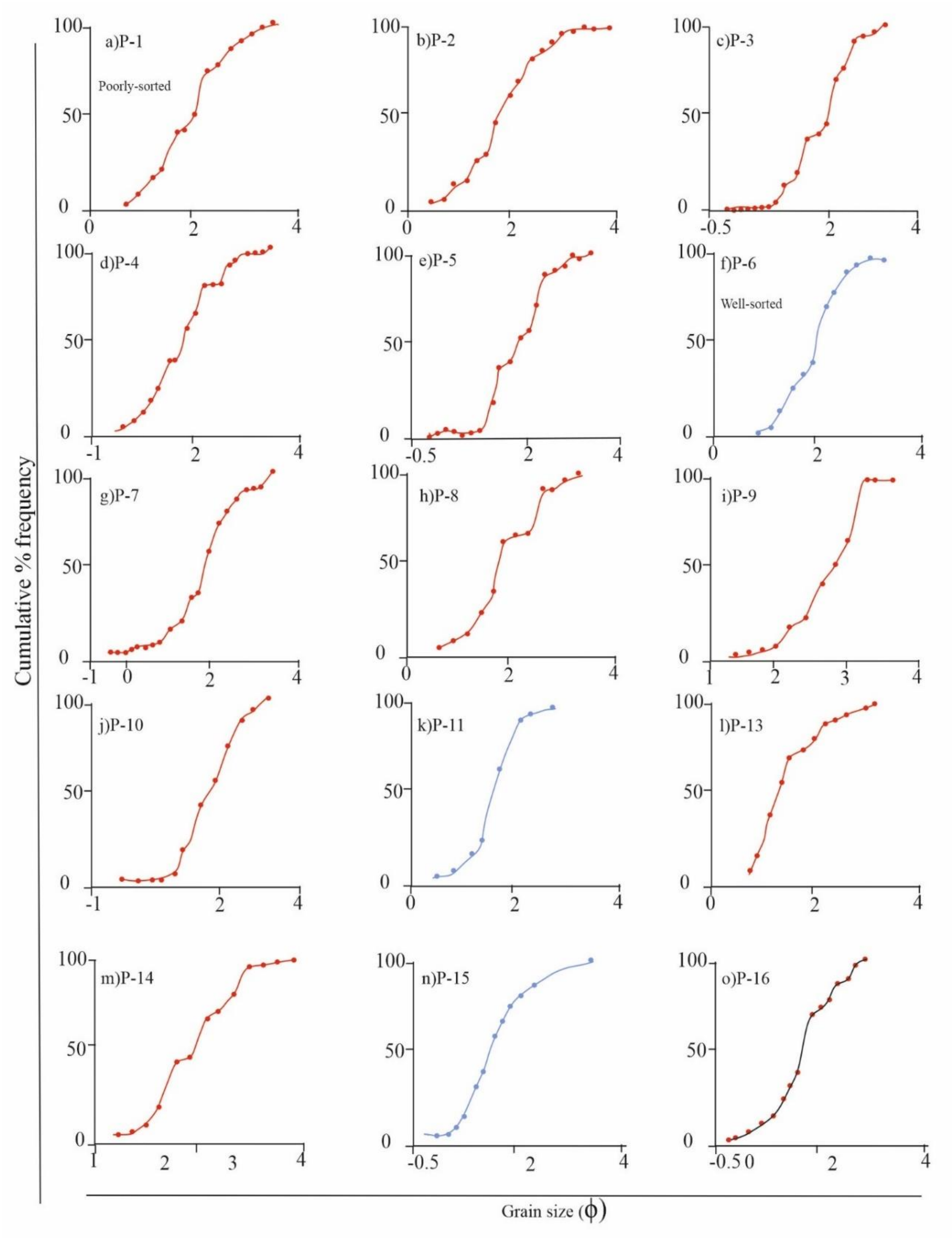

Figure 3. Cumulative present frequency curves of the sandstones

Table 2. Grain size statistical parameters of the studied sandstones

Sample	**ϕ1**	**ϕ 5**	**ϕ 16**	**ϕ 25**	**ϕ 50**	**ϕ 75**	**ϕ 84**	**ϕ 95**	**Mz**	**σ_1**	**Sk**
P-1	0.85	1.00	1.15	1.40	2.01	2.20	2.65	3.01	1.93	0.67	-0.07
P-2	0.45	0.75	1.01	1.25	1.75	2.11	2.51	2.98	1.75	0.71	0.01
P-3	-0.01	1.20	1.81	1.85	2.25	2.60	2.82	3.10	2.28	0.56	0.10
P-4	-0.30	-0.25	1.10	1.20	1.75	2.01	2.50	2.81	1.78	0.80	0.04
P-5	-0.02	1.25	1.40	1.45	1.80	2.20	2.25	2.80	1.82	0.44	0.03
P-6	1.01	1.15	1.40	1.61	2.20	2.52	2.55	3.12	2.01	0.58	-0.20
P-7	-0.5	0.00	1.11	1.25	1.95	2.10	2.35	3.10	1.83	0.78	-0.19
P-8	0.71	0.75	1.15	1.25	1.62	2.21	2.51	3.01	1.75	0.68	0.16
P-9	1.25	1.80	2.20	2.50	2.85	3.11	3.25	3.30	2.77	0.49	-0.13
P-10	-0.12	1.41	1.65	1.70	1.85	2.20	2.42	2.81	1.97	0.43	0.21
P-11	0.50	0.75	1.00	1.51	1.70	1.95	2.11	2.55	1.61	0.54	-0.14
P-13	0.75	0.82	1.02	1.05	1.25	2.01	2.25	3.05	1.50	0.65	0.27
P-14	1.30	1.85	2.01	2.45	2.91	3.08	3.15	1.20	2.68	0.27	-0.03
P-15	-0.15	-0.10	-0.01	0.10	0.85	1.75	2.40	3.11	1.08	1.07	0.14
P-16	-0.25	-0.11	0.50	0.95	1.40	1.90	2.13	2.50	1.33	0.79	-0.06

Table 3. Grain size scale for sandstone (Udden and Wentworth, [48].

mm	ϕ	Class terms and Rock terms	This study	
			Min. value	Max. value
2	-1	Very coarse sandstone		
1.68	-0.75			
1.41	-0.5			
1.19	-0.25			
1	0.0			
0.84	0.25	Coarse sandstone		
0.71	0.5			
0.59	0.75			
0.50	1			
0.42	1.25	Medium sandstone		1.93
0.35	1.5			
0.30	1.75			
0.25	2			
0.210	2.25	Fine sandstone	2.77	
0.177	2.5			
0.149	2.75			
0.125	3.0			
0.105	3.25	Very fine sandstone		
0.088	3.5			
0.074	3.75			
0.063	4			

4.2.4. Graphic skewness (Sk)

Graphic skewness is a measure of the symmetry of the dispersion and visually is best in the smoothed frequency curve. If there is a fine tail, then sediment is thought to be positive (excess fine materials), if there is a coarse tail then the skew is negative (excess coarse materials). If there is no skew, the distribution will be symmetrical [48]. In addition, skewness indicates the type of deposition process. River sands, for example, are commonly positively skewed, and beach sands and some desert sands are negatively skewed.

In the studied sandstone samples, Sk values change from -0.2 to 0.16 ϕ, indicating coarse-skewed (positively skewed) and fine-skewed (negatively skewed) (Table 5). Figure 2 shows that sandstone samples P-1, P-3, P-4, P-6, P-7, P-9 have a coarse-skewed and the samples P-2, P-5, P-8, P-10, P-11, P-13, P-14, P-15, and P-16 are fine-skewed. This indicates that material was transported into the basin from both the distant source and the near source. Usually, the sediment becomes more coarse-skewed (coarser-grained) along its sediment transport from near, whereas the sediment becomes more fine-skewed (finer-grained) along its sediment transport from away [49].

Table 4. Classification scale for sorting [48].

σ_1	Classification	This study	
		Mean Min	Mean Max
<0.35 ϕ	Very well sorted		0.27
0.35 - 0.50 ϕ	Well sorted		
0.50 – 0.71 ϕ	Moderately well sorted		
0.71 – 1.0 ϕ	Moderately sorted		
1.0 – 2.0 ϕ	Poorly sorted	1.07	
2.0 – 4.0 ϕ	Very poorly sorted		
>4.0 ϕ	Extremely poorly sorted		

Table 5. Classification scale for graphic skewed [48].

Sk	Classification	This study	
		Mean Min	Mean Max
1.0 – 0.30 ϕ	Strongly fine skewed		
0.30 - 0.10 ϕ	Fine skewed	0.16	
0.10 – -0.10 ϕ	Near symmetrical		
-0.10 – -0.30 ϕ	Coarse skewed		-0.20
-0.30 – -1.0 ϕ	Strongly coarse skewed		

4.3. Grain morphology

Grain morphology is defined by three approaches roundness, sphericity, and shape. The shape of the grain is measured by diverse ratios of short, intermediate, and long axes and defined four classes according to these ratios (disc-shaped, spherical, bladed, and rod-shaped). Roundness is related to the curvature of the corners of the grain and is determined by six classes (very angular, angular, subangular, subrounded, rounded, and well-rounded [50]. Sphericity is a measure of how similar the grain shape is to a spherical shape. For environmental and transport distance interpretations, the roundness measures are very important, but sphericity and shape do not matter much.

The roundness of the examined sandstones was determined as subangular, subrounded, and rounded (Figure 4). This confirms that the studied sandstones received material from two different sources since the degree of roundness increases with reworking and increasing transport distance. Rounded grains were transported from a distant source and surrounded and subangular grains were transported from a close-range source.

5. Textural maturity

Texturally mature sandstones are those with little matrix, subrounded to rounded grains, and moderate to good sorting and texturally super mature sandstones are those with no matrix, well-rounded grains, and very good sorting, whereas texturally immature sandstones are those with many matrices, angular grains, and o poor sorting [48].

In this study, the sandstone samples are with little matrix, subangular, subrounded to rounded grains, and very well sorted to poorly sorted. Therefore, the studied samples change between texturally mature and immature sandstones, indicating bivariate sources for sandstones one close to the basin and the other farther away.

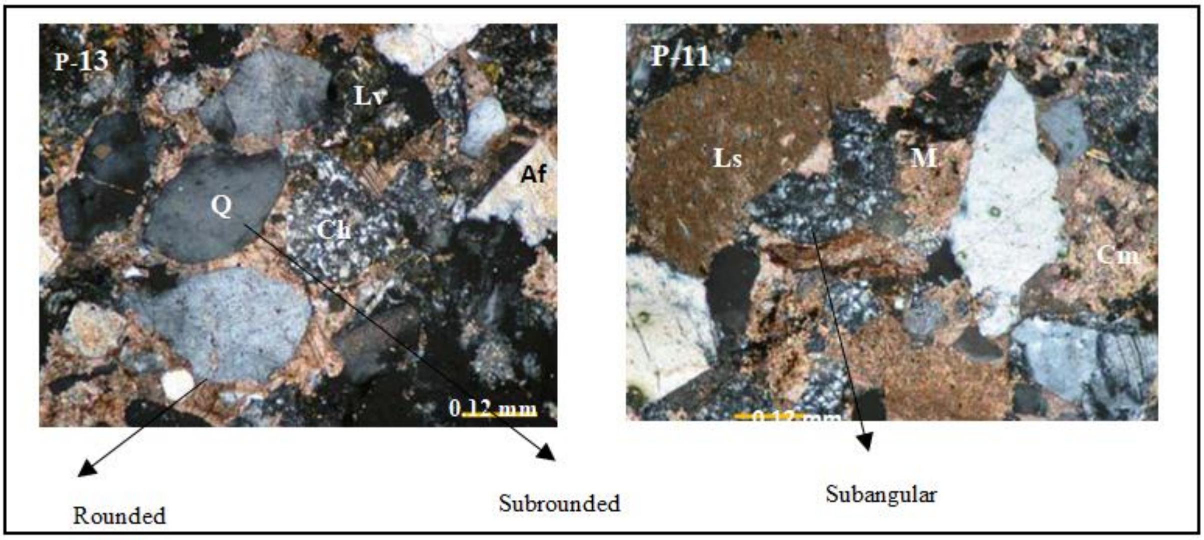

Figure 4. Microscopic view of selected same samples of sandstones (Qm: Monocrystalline quartz, Af: Alkali feldspar, Lv: Volcanic rock fragment, Ls: Sedimentary rock fragment, M: Matrix, Cm: Cement, Ch: Chert, Op: Opaque mineral)

6. Conclusions

1. This study brings to light the textural features of Eocene-aged sandstone can give clues to understanding its source area distance and whether it is texturally mature. The sequence with a measured thickness of 280 m is constituted of conglomerate, sandstone, marl, limestone, and tuff.
2. According to the mean grain size (Mz) of the investigated sandstones are classified as medium-grained to fine-grained sandstone. In addition, it is determined that the grain size of monocrystalline quartz is very coarse sand, polycrystalline quartz is very fine sand to very coarse sand, alkali feldspar is very fine sand to very coarse sand, plagioclase is very fine sand to fine sand, volcanic rock fragments is very fine sand to very coarse sand, and sedimentary rock fragments is coarse sand to very fine sand.
3. The standard deviation (σ_1) values, frequencies, and cumulative frequency curve indicate that the sorting of sandstone samples is very well-sorted to poorly sorted. According to skewed (Sk) values, it is said that the sandstone samples are coarse-skewed to fine-skewed.
4. The morphology of the investigated sandstones was determined as subangular, subrounded, and rounded.
5. Finally, Eocene-age sandstones have ranged from mature to immature texture, exhibiting bivariate sources for sandstones one close to the basin and the other farther away.

Acknowledgments

I would like to thank the editor and anonymous reviewer for their contributions to the manuscript.

References

[1] Tucker, M.E. Sedimentary Petrology. Blackwell Scientific Publ., Oxford, 1991; 10–19p.
[2] Zeng, D.Y., Wu, S-X. Principal component analysis of textural characteristics of fluvio-lacustrine sandstones and controlling factors of sandstone textures. Geological Magazine 2021; DOI:10.1017/S0016756821000418.
[3] Srivastava, A.K., Ingle, P.S., Lunge, H.S., Khare, N. Grain-size characteristics of deposits derived from different glaciogenic environments of the Schirmacher Oasis, East Antarctica. Geologos 2012; 18(4): 251–66.
[4] Baiyegunhi, C., Liu, K., Gwavava, O. Grain size statistics and depositional pattern of the Ecca Group sandstones, Karoo Supergroup in the Eastern Cape Province, South Africa. Open Geoscience 2017; 9: 554–76.
[5] Baiyegunhi, T.L., Liu, K., Gwavava, O., Baiyegunhi, C. Textural characteristics, mode of transportation and depositional environment of the Cretaceous sandstone in the Bredasdorp Basin, off the south coast of South Africa: Evidence from grain size analysis. Open Geoscience 2020; 12: 1512–1532.
[6] Blott, S. J., Pye K., Radistat, A. Grain size distribution and statistics package for the analysis of unconsolidated sediments. Earth Surf Process Land 2001; 26: 1237–48.
[7] Saydam Eker, C. Petrography and geochemistry

of Eocene sandstones from eastern Pontides (NE Turkey): Implications for source area weathering, provenance, and tectonic setting. Geochemistry International, 2012; 50(8): 683–701.
[8] Saydam Eker, C. Organic geochemical characteristics and depositional environments of the Eocene deposits in the Eastern Black Sea Region, NE Turkey. Energy Sources, Part A: Recovery, Utilization, and Environmental Effects 2013; 35: 413–425.
[9] Aydınçakır, E., Şen, C. Petrogenesis of the postcollisional volcanic rocks from the Borçka (Artvin) area: implications for the evolution of the Eocene magmatism in the Eastern Pontides (NE Turkey). Lithos 2013; 172–173: 98–117.
[10] Aydıncakır, E. The petrogenesis of Early Eocene non-adakitic volcanism in NE Turkey: constraints on the geodynamic implications. Lithos 2014; 208–209: 361–377.
[11] Saydam Eker, Ç., Akpınar, İ., Sipahi, F. Organic geochemistry and element distribution in coals formed in Eocene Lagoon facies from the Eastern Black Sea Region, NE Turkey. Turkish Journal of Earth Science 2016; 25: 467–489.
[12] Kaygusuz, A., Şahin, K. Petrographical, geochemical and petrological characteristics of Eocene volcanic rocks in the Mescitli area, Eastern Pontides (NE Turkey), Journal of Engineering Research and Applied Science 2016; 5 (2): 473–486.
[13] Akaryalı, E., Akbulut, K. Constraints of C–O–S isotope compositions and the origin of the Ünlüpınar volcanic-hosted epithermal Pb–Zn ± Au deposit, Gümüşhane, NE Turkey. Journal of Asian Earth Sciences 2016; 117: 119–134.
[14] Aydınçakır, E., Yücel, C., Ruffet, G., Gücer, M.A., Akaryalı, E., Kaygusuz, A. Petrogenesis of post-collisional Middle Eocene volcanism in the Eastern Pontides (NE, Turkey): Insights from geochemistry, whole-rock Sr-Nd-Pb isotopes, zircon U-Pb and ^{40}Ar-^{39}Ar geochronology, Chemie der Erde – Geochemistry 2022; 82 (2): 125871.
[15] Kaygusuz, A., Merdan Tutar, Z., Yücel, C. Mineral chemistry, crystallization conditions and petrography of Cenozoic volcanic rocks in the Bahçecik (Torul/Gümüşhane) area, Eastern Pontides (NE Turkey). Journal of Engineering Research and Applied Science 2017; 6 (2): 641–651.
[16] Topuz, G., Altherr, R., Kalt, A., Satır, M., Werner, O., Schwarz, W. Aluminous granulites from the Pulur complex, NE Turkey: a case of partial melting, efficient melt extraction and crystallization. Lithos 2004; 72: 183–207.
[17] Topuz, G., Altherr, R., Wolfgang, S., Schwarz, W.H., Zack, T., Hasanözbek, A., Mathias, B., Satır, M., Şen, C. Carboniferous high-potassium I-type granitoid magmatism in the Eastern Pontides: The Gümüşhane Pluton (NE Turkey), Lithos 2010; 116: 92–110.
[18] Dokuz, A. A slab Detachment and delamination model for the generation of Carboniferous high-potassium i-type magmatism in the Eastern Pontides, NE Turkey: Köse Composite Pluton. Godwana Research 2011; 19: 926–944.
[19] Ustaömer, T., Robertson, A.H.F., Ustaömer, P.A., Gerdes, A., Peytcheva, I. Constraints on Variscan and Cimmerian magmatism and metamorphism in the Pontides (Yusufeli–Artvin area), NE Turkey from U–Pb dating and granite geochemistry. In: Robertson, A.H.F., Parlak, O., Ünlügenç, U.C., (eds.), Geological development of Anatolia and the easternmost Mediterranean Region. Geological Society of London Special Publications 2013; 372: 49-74.
[20] Kaygusuz, A., Arslan, M., Siebel, W., Sipahi, F., İlbeyli, N. Geochronological evidence and tectonic significance of Carboniferous magmatism in the southwest Trabzon area, eastern Pontides, Turkey. International Geology Rew 2012; 54 (15): 1776–1800.
[21] Vural, A., Kaygusuz, A. Petrology of the paleozoic plutons in Eastern pontides: artabel pluton (Gümüşhane, NE Turkey). Journal of Engineering Research and Applied Science 2019; 8 (2): 1216–1228.
[22] Aydınçakır, E., Gündüz, R., Yücel C. Emplacement conditions of magma(s) forming Jurassic plutonic rocks in Gümüşhane (Eastern Pontides, Turkey). Bulletin of the Mineral Research and Exploration 2020; 162: 175–196.
[23] Saydam Eker, C., Sipahi, F., Kaygusuz, A. Trace and rare earth elements as indicators of provenance and depositional environments of Lias cherts in Gumushane, NE Turkey. Chemie Der Erde-Geochemistry 2012; 72 (2): 167–177.
[24] Saydam Eker, C., Sipahi, F., Akpinar, İ. Organic maturity and hydrocarbon potential of Liassic coals from the Eastern Pontides, NE Turkey. Energy Sources, Part A: Recovery, Utilization, and Environmental Effects 2015; 37: 1260–1267.
[25] Saydam Eker, Ç., Arı, U.V. Comparison of sandstone and mudstone with different methods for assessing toxic element contamination in the Early–Middle Jurassic sediments of Gümüşhane (NE Turkey). Environmental Earth Sciences 2020a; 79: 444.
[26] Saydam Eker, Ç., Arı, U.V. Geochemistry of the Middle Jurassic sediments in Gümüşhane, north-

eastern Turkey: implications for weathering and provenance. Geological Journal 2020b; 55: 4954–4976.

[27] Kara-Gülbay, R., Kırmacı, M.Z., Korkmaz, S. Organic Geochemistry and Depositional Environment of the Aptian Bituminous Limestone in the Kale Gümüşhane Area (NE-Turkey): an Example for Lacustrine Deposits on the Platform Carbonate Sequence. Organic Geochemistry 2012; 49: 6–17.

[28] Özyurt, M. Origin of dolomitization in Upper Jurassic-Lower Cretaceous platform carbonates (Berdiga Formation) in the Gümüşhane area PhD, 2019; Karadeniz Technical University, Trabzon, Turkey

[29] Saydam Eker, C., Korkmaz, S. Source Rock Characteristics and Hydrocarbon Potential of the Late Cretaceous Deposits in the Eastern Black Sea Region, NE Turkey 2008; 30: 1141–1151.

[30] Saydam Eker, C., Korkmaz, S. Mineralogy and whole-rock geochemistry of late Cretaceous sandstones from the eastern Pontides (NE Turkey). Neues Jahrbuch Für Mineral Abhandlungen, 2011; 188(3): 235–256.

[31] Sipahi, F., Kaygusuz, A., Saydam, Eker, Ç., Vural, A., Akpınar, İ. Late Cretaceous Arc Igneous Activity: The Eğrikar Monzogranite Example. International Geology Review 2018; 60: 382–400.

[32] Kaygusuz, A., Arslan, M., Temizel, İ., Yücel, C., Aydınçakır, E., U–Pb zircon ages and petrogenesis of the Late Cretaceous I-type granitoids in arc setting, Eastern Pontides, NE Turkey, Journal of African Earth Sciences 2021; 174: 104040.

[33] Kaygusuz, A., Saydam Eker, Ç. Geochemical features and petrogenesis of Late Cretaceous subduction-related volcanic rocks in the Değirmentaşı (Torul/Gümüşhane) area, Eastern Pontides (NE Turkey). Journal of Engineering Research and Applied Science 2021; 10 (1): 1689–1702.

[34] Köprübaşı, N., Şen, C., Kaygusuz, A. Doğu Pontid Adayayı Granitoyidlerinin Karşılaştırılmalı Petrografik ve Kimyasal Özellikleri, KD Türkiye, Uygulamalı Yerbilimleri Dergisi 2000; 1: 111–120.

[35] Karslı, O., Dokuz, A., Uysal, İ., Aydın, F., Kandemir, R., Wijbrans, R.J. Generation of the early Cenozoic adakitic volcanism by partial melting of mafic lower crust, Eastern Turkey: implications for crustal thickening to delamination. Lithos 2010; 114: 109–120.

[36] Kaygusuz, A., Siebel, W., Şen, C., Satır, M. Petrochemistry and petrology of I-type granitoids in an arc setting: The Composite Bayburt Pluton, Eastern Pontides, NE Turkey. International Journal of Earth Sciences 2008; 97: 739–764.

[37] Eyüboğlu Y., Dudas, F.O., Thorkelson, D., Zhu, D.C., Liu, Z., Chatterjee, N., Yi, K., Santosh, M. Eocene Granitoids of Northern Turkey: Polybaric magmatism in an evolving arc-slab window system, Gondwana Research 2017; 50: 311–345.

[38] Kaygusuz, A., Yücel, C., Arslan, M., Temizel, İ., Yi, K., Jeong, Y-J., Siebel, W., Sipahi, F. Eocene I-type magmatism in the Eastern Pontides, NE Turkey: Insights into magma genesis and magma-tectonic evolution from whole-rock geochemistry, geochronology and isotope systematics, International Geology Review 2020; 62 (11): 1406–1432.

[39] Vural, A., Kaygusuz, A. Geochronology, petrogenesis and tectonic importance of Eocene I-type magmatism in the Eastern Pontides, NE Turkey. Arabian Journal of Geosciences 2021; 14: 467. doi.org/10.1007/s12517-021-06884-z.

[40] Kaygusuz, A., Arslan, M., Siebel, W., Şen, C. Geochemical and Sr-Nd isotopic characteristics of post-collisional calc-alkaline volcanics in the Eastern Pontides (NE Turkey) Turkish Journal of Earth Sciences 2011; 20: 137–159.

[41] Kaygusuz, A., Yücel, C., Aydınçakır, E., Gücer, M.A., Ruffet, G. Petrogenesis of the Middle Eocene calc-alkaline volcanic rocks in the Bayburt area, Eastern Pontides (NE Turkey): Implications for magma evolution in extension-related setting. Mineralogy and Petrology 2022; 116: 379–399.

[42] Saydam Eker, Ç. Geochemical and isotopic characteristics of stream and terrace sediments of the Harsit Stream, NE Turkey. Geochemistry Explorer Environment Analysis, 2017; 17(4): 279–296.

[43] Saydam Eker, Ç. Distinct contamination indices for evaluating potentially toxic element levels in stream sediments: a case study of the Harşit Stream (NE Turkey). Arabian Journal of Geosciences 2020a; 13: 1175.

[44] Güven, I.H. 1/100.000 scaled geological map series of Turkey. No.57-60. MTA Publication, Ankara, 1993.

[45] Johnson M.R. Thin section grain size analysis revisited. Sedimentology. 1994; 41: 985–99.

[46] Saydam Eker, Ç. Sedimanter Petrographic Properties of Eocene Sandstones and an Approach to Provenance According to Plate Tectonics in the Gümüşhane Region. Geological Bulletin of Turkey 2008; 51(3): 131–148.

[47] Saydam Eker, Ç. Potentially toxic element levels in the Eocene sandstones from Gümüşhane

area (NE Turkey). Journal of Engineering Research and Applied Science 2020; 9(1): 1374–1385.
[48] Folk, R., L. Petrology of Sedimentary Rocks, Hemphill Publishing Company Austin, Texas 78703, 1980; p.16–30
[49] McLaren, P., Bowles, D. The Effects of Sediment Transport on Grain-Size Distributions. Journal of Sedimentary Research 1985; 55: 457–470.
[50] Pettijohn, F. J., Potter, P. E., Siever, R. Sand and Sandstone, 2nd Edition (Springer, Berlin–Heidelberg–New York), 1987.